LEARNING LINEARITY IN AUDIO CONSISTENCY AUTOENCODERS VIA IMPLICIT REGULARIZATION

Bernardo Torres*

Manuel Moussallam[†]

Gabriel Meseguer-Brocal †

*LTCI, Telecom Paris, Institut Polytechnique de Paris

†Deezer Research

ABSTRACT

Audio autoencoders learn useful, compressed audio representations, but their non-linear latent spaces prevent intuitive algebraic manipulation such as mixing or scaling. We introduce a simple training methodology to induce linearity in a high-compression Consistency Autoencoder (CAE) by using data augmentation, thereby inducing homogeneity (equivariance to scalar gain) and additivity (the decoder preserves addition) without altering the model's architecture or loss function. When trained with our method, the CAE exhibits linear behavior in both the encoder and decoder while preserving reconstruction fidelity. We test the practical utility of our learned space on music source composition and separation via simple latent arithmetic. This work presents a straightforward technique for constructing structured latent spaces, enabling more intuitive and efficient audio processing.

Index Terms— audio, compression, diffusion, source separation

1. INTRODUCTION

Modern Autoencoders (AEs) can achieve excellent reconstruction quality at high compression rates at the expense of complex, entangled latent spaces. For applications where input space manipulation is desirable from within the compressed space, recent research has proposed either task-specific adaptors for pre-trained models or redesigning the autoencoder to preserve key structural properties, such as equivariance to spatial transformations [1–3]). This work follows the latter approach.

For certain applications in audio, linearity (Figure 1) is a desirable property. A linear map fulfills two properties: (I) Homogeneity: scaling the input by a value scales the output by the same value; and (II) Additivity: the map preserves addition. As processing large audio datasets in the latent space becomes more prevalent, direct mixing and volume adjustment in this space can improve efficiency by reducing redundant encoding and decoding. Additionally, as downstream tasks such as audio generation and source separation can benefit from composition via latent arithmetic, better interpretability may be achieved when working on a linear space.

This work presents a training methodology for constructing an approximately linear compressed audio representation that enables intuitive manipulation, where simple algebraic operations in the latent space correspond directly to mixing and scaling in the audio domain. The method employs implicit regularization through data augmentation, without modifying the model architecture or objective. The approach is demonstrated with the Music2Latent architecture [4], a Consistency Autoencoder (CAE) that achieves high-quality, single-step reconstruction and a $64\times$ compression rate for 44.1 kHz audio.

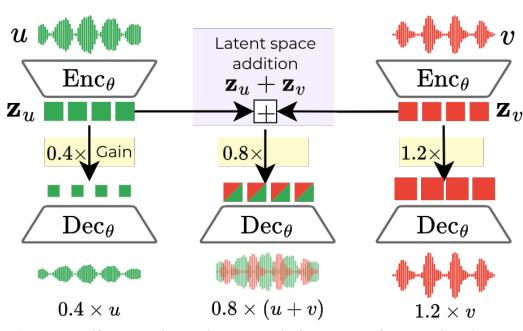


Figure 1: In a linear decoder, applying a gain to the latent vector scales the output by the same gain (homogeneity), and summing latents corresponds to a sum in the audio domain (additivity).

Our main contributions are: (I) An unsupervised, data-augmentation-based training procedure that induces approximate linearity in a high compression AE, with no extra loss terms; (II) Validation on a state-of-the-art CAE for music and speech, showing linearity in both encoder and decoder with no loss of reconstruction quality; (III) Practical utility shown on oracle source separation via simple latent arithmetic. Code and model weights are available online ¹.

2. BACKGROUND

2.1. Audio processing in the latent space

There is a growing interest in manipulating audio by training task-specific modules which operate directly in the latent space of a pre-trained AE, with applications in source separation [5], speech enhancement [6, 7], upsampling and upmixing [8], filtering [9], and generative modelling [10–12]. Some works retrain AEs for specific objectives, such as source disentanglement [13] or separation via latent masking [14]. In contrast, our work focuses on training an AE to have desirable, task-agnostic structural properties. This enables direct and efficient audio manipulation and can serve as a strong foundation for these downstream applications.

2.2. Diffusion and Consistency models

Denoising Diffusion Probabilistic Models [15] and score-based models [16] have achieved great success in generative modeling, where the goal is to estimate the underlying data distribution from samples. These models define a forward process that gradually adds noise to data and learn a reverse process to denoise it using a neural network. Sampling typically requires an iterative procedure with many steps to generate a clean sample. Consistency Models (CMs) [17] accelerate this process by mapping any point along the trajectory defined by

[★]Work done during an internship at Deezer Research

¹www.github.com/bernardo-torres/linear-autoencoders.

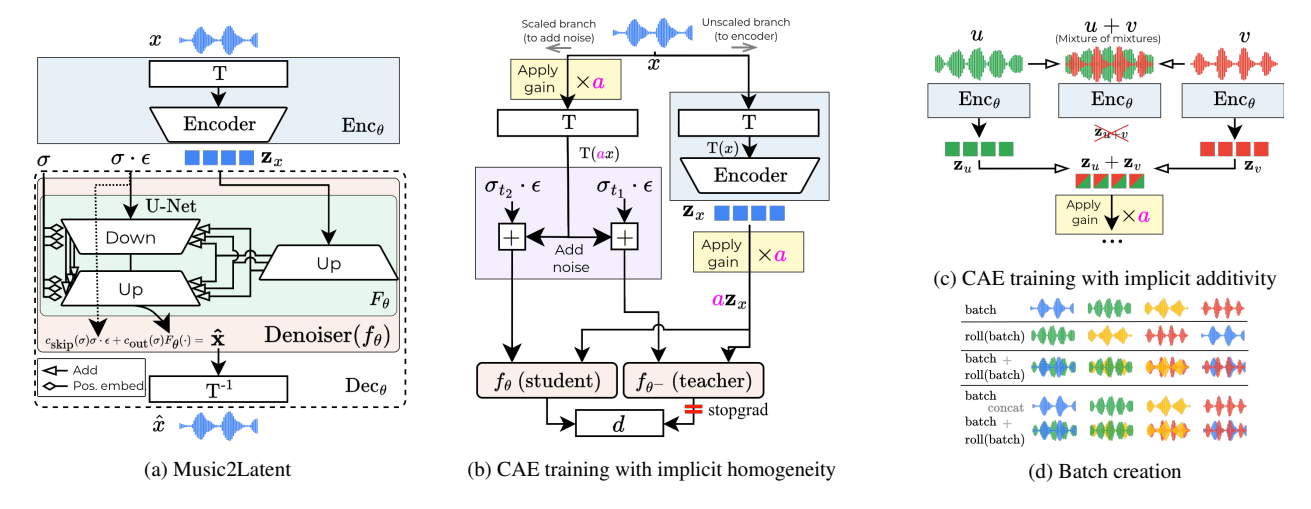


Figure 2: (a): Music2Latent CAE architecture. The decoder is a denoising U-Net and the latent is introduced to it at every resolution level after learned upsampling. (b): Proposed CAE training trick to implicitly enforce homogeneity in the decoder. (c): Proposed trick to enforce additivity, applied when the input is an artificial mixture. (d): Batch creation procedure with artificial mixtures of mixtures.

the probability flow ordinary differential equation [16] directly to the origin (the clean data point), enabling single-step generation. When trained from scratch, the process is called Consistency Training (CT), in which a "student" denoiser network (f_{θ}) is trained to match the output of a "teacher" (f_{θ^-}) , which itself denoises a less corrupted version of the same data point. In improved Consistency Training (iCT) [18], the teacher is updated with the same parameters θ as the student but detached from the computational graph $(\theta^- \leftarrow \text{stopgrad}(\theta))$.

2.3. High-Fidelity Audio Autoencoders

In audio, popular AEs include Neural Audio Codecs [19], which compress audio into a set of discrete tokens, and Variational Autoencoders (VAEs) [20], which have seen significant success in generative modeling. However, both frameworks require complex, multi-stage training with adversarial objectives [21] to achieve high-quality reconstructions. Diffusion Autoencoders (DiffAEs) [10, 22–25] enable high-fidelity reconstruction by replacing the deterministic decoder with a conditional diffusion model. Notable examples in audio include [10] and Music2Latent [4, 26]. A specific instance of DiffAEs is the CAE [4, 26], where the decoder is a CM, enabling decoding in one step. DiffAEs can be trained with a single diffusion/CT objective [4, 22, 24]. High-quality decoding has been linked to the capacity of sampling details at inference-time, since the decoder acts as a denoiser instead of an upsampler, which also reduces the amount of unnecessary information to be encoded in the latent [23, 25].

3. METHOD

Let $\mathcal{M} \subset [-1,1]^T$ be the space of audio signals of length T of interest and $\mathcal{Z} \subset \mathbb{R}^{N \times F}$ be a lower-dimensional latent space induced by encoder $\mathrm{Enc}_\theta : \mathcal{M} \to \mathcal{Z}$ and decoder $\mathrm{Dec}_\theta : \mathcal{Z} \to \mathcal{M}$, with dimensions N, F defined by the compression factor. We train $(\mathrm{Enc}_\theta, \mathrm{Dec}_\theta)$ with CAE training under the constraint that Dec_θ is approximately linear (Figure 1), i.e., it satisfies the following properties:

Property 1 (Homogeneity).

$$\operatorname{Dec}_{\theta}(\mathbf{a} \cdot \mathbf{z}_x) \approx \mathbf{a} \cdot \operatorname{Dec}_{\theta}(\mathbf{z}_x), \quad \forall \mathbf{z}_x \in \mathcal{Z}, \mathbf{a} \in \mathbb{R}$$
 (1)

Property 2 (Additivity).

$$\operatorname{Dec}_{\theta}(\mathbf{z}_{u} + \mathbf{z}_{v}) \approx \operatorname{Dec}_{\theta}(\mathbf{z}_{u}) + \operatorname{Dec}_{\theta}(\mathbf{z}_{v}), \quad \forall \mathbf{z}_{u}, \mathbf{z}_{v} \in \mathcal{Z}$$
 (2)

We postulate that approximate linearity can be achieved by a simple data augmentation scheme, without the need to change model or loss function. Our approach is in theory model-agnostic and can be applied to any AE, and in this work we apply it on a CAE architecture for audio [4], which offers $64\times$ compression and high-quality reconstruction with a single training objective.

3.1. Model architecture

Our model (Lin-CAE) follows the Music2Latent architecture [4], illustrated in Figure 2(a). We recall the main components here for clarity, but we refer the reader to [4] for the full details.

CAE Denoiser representation space: We use a complex-valued Short-Time Fourier Transform (STFT) followed by the invertible amplitude scaling Amp: $\mathbb{C} \to \mathbb{C} = \beta |c|^{\alpha} e^{i \angle(c)}$ (with $\alpha = 0.65$ and $\beta = 0.34$) from previous work in complex STFT diffusion [4,27,28], which scales the amplitudes in the STFT to roughly [-1,1] while boosting the high frequencies. We define $T(x) = \mathrm{Amp}(\mathrm{STFT}(x))$ as the transform which maps from waveform to CM input space.

Decoder: $\operatorname{Dec}_{\theta}$ is composed of a U-Net-based denoiser f_{θ} and the inverse transform $\operatorname{T}^{-1}(\mathbf{x})$. The denoiser reconstructs $\mathbf{x} = \operatorname{T}(x)$ from a noise-corrupted version $\mathbf{x}_{\sigma} = \mathbf{x} + \sigma \boldsymbol{\epsilon} \ (\boldsymbol{\epsilon} \sim \mathcal{N}(0,I))$, conditioned on the latent \mathbf{z}_x and the noise level σ . \mathbf{z}_x is upsampled with a dedicated network mirroring the U-Net's upsampling block and added to each layer of the U-Net. Noise level information is added to every layer via positional embeddings. f_{θ} is parameterized by a noise prediction network F_{θ} with a skip connection weighted by coefficients $(c_{\text{skip}}, c_{\text{out}})$ that depend on σ [29], which additionally enforces the boundary condition necessary for CT [4, 17, 18]:

$$f_{\theta}(\mathbf{x}_{\sigma}, \sigma, \mathbf{z}_{x}) = c_{\text{skip}}(\sigma)\mathbf{x}_{\sigma} + c_{\text{out}}(\sigma)F_{\theta}(\mathbf{x}_{\sigma}, \sigma, \mathbf{z}_{x})$$
(3)

During inference, decoding starts from pure noise and the clean signal is reconstructed in a single step conditioned on z_x .

Encoder: $\operatorname{Enc}_{\theta}$ consists of the amplitude transform T followed by a network that mirrors the U-Net's downsampling blocks.

3.2. Learning Linearity in CAEs via Implicit Regularization

Implicit homogeneity: Inspired by [1], we apply a random positive gain (a) to the latent and task the decoder to reconstruct a scaled

version of the input (ax). The adapted CT training, depicted in Figure 2(b), uses two parallel pathways. $\operatorname{Enc}_{\theta}$ encodes unscaled x to obtain \mathbf{z}_x . Then, the denoiser (f_{θ}) receives a noisy scaled input $(T(ax) + \sigma \epsilon)$ conditioned on the scaled latent $(a\mathbf{z}_x)$. a is never provided as an explicit input to any part of the model, so $\operatorname{Dec}_{\theta}$ must learn to infer the correct output scale from the magnitude of the conditioning latent. If a = 1, we recover the original CAE training.

Implicit additivity: Inspired by Mixit [30], we augment our data by creating artificial mixes from pairs of elements (u, v) randomly selected from the training set. When decoding, we replace the true latent of the artificial mix $(\operatorname{Enc}_{\theta}(u+v))$ with the sum of the latents of the individual signals: $\mathbf{z}' \leftarrow (\mathbf{z}_u + \mathbf{z}_v)$, where $(\mathbf{z}_u = \operatorname{Enc}_{\theta}(u), \mathbf{z}_v = \operatorname{Enc}_{\theta}(v))$, as illustrated in Figure 2(c). The denoiser is thus conditioned on \mathbf{z}' and tasked with denoising $T(\mathbf{a}(u+v)) + \sigma \epsilon$). We create mixtures from each training batch by concatenating it with a version of itself that has been circularly shifted by one position and summed with the original (Figure 2(d)).

3.3. Training

With the modifications described in Section 3.2 highlighted in color, we train the model under the CT objective \mathcal{L}_{CT} [4, 17, 18], which minimizes the distance between the denoised output of a teacher (f_{θ^-}) and student (f_{θ}) models $(\theta^- \leftarrow \text{stopgrad}(\theta))$ for noisy inputs at two different noise levels, σ_{t_1} and σ_{t_2} .

$$\mathcal{L}_{\text{CT}} = \mathbb{E}_{\mathbf{x}, \boldsymbol{\epsilon}, t_1, \boldsymbol{a}} \left[\lambda \cdot d \left(f_{\theta}(\mathbf{T}(\boldsymbol{a}\boldsymbol{x}) + \sigma_{t_2} \boldsymbol{\epsilon}, \sigma_{t_2}, \boldsymbol{a}\mathbf{z}'), \right. \right.$$

$$\left. f_{\theta^{-}}(\mathbf{T}(\boldsymbol{a}\boldsymbol{x}) + \sigma_{t_1} \boldsymbol{\epsilon}, \sigma_{t_1}, \boldsymbol{a}\mathbf{z}') \right) \right],$$

$$(4)$$

where \mathbf{z}' is either \mathbf{z}_x or $\mathbf{z}_u + \mathbf{z}_v$ depending on whether the input waveform is sampled from the training set or is an artificial mixture $(x=u+v), \epsilon \sim \mathcal{N}(0,I)$ is a shared noise direction, $\lambda(\sigma_{t_1},\sigma_{t_2})=\frac{1}{\sigma_{t_2}-\sigma_{t_1}}$ is a weighting function designed to give higher weights to smaller noise increments [18]. We sample time steps $t_1 \in [0,1]$ and corresponding noise levels σ_{t_1,t_2} following [4], with $t_2=t_1+\Delta_{t_k}$, where Δ_{t_k} depends on the training step k and decays over training $(\Delta t_k = \Delta t_0^{\frac{k}{K}(e_K-1)+1}, \Delta t_0 = 0.1, e_K = 2.0)$. d is the Pseudo-Huber loss [31]: $d(x,y) = \sqrt{|x-y|^2+c^2}-c$, with c=5.4e-4.

Training details: We train all models for 800K steps with a batch size of 20 before mixture creation (final batch size of 40). Training takes ≈ 8 days on 1 L40S GPU. The models are optimized with RAdam with learning rate $\in [10^{-4}, 10^{-6}]$ (linear warmup for 10K steps, cosine decay for the rest). We track an Exponential Moving Average (EMA) of the model parameters θ to be used for inference, updated every 10 steps.

Homogeneity gains are sampled from a uniform distribution in $[a_{\min},a_{\max}]$ and applied with probability 0.8 to each sample in the batch. If |a|<0.05, we set it to 0. Gains are clipped so that the maximum absolute value of the waveform does not exceed 1. We anneal gain range from $(a_{\min}=0,a_{\max}=3)$ to no gain (1,1) over training using a piecewise cosine schedule. Gain boundaries are defined as: $a_{\min}(k)=1-\cdot C(k)$ and $a_{\max}(k)=1+2\cdot C(k)$, where C(k) is 1 if $k\leq 0.2K$, 0 if $k\geq 0.9K$, and follows a cosine decay $C(k)=\frac{1}{2}(1+\cos(\pi\cdot\frac{k-0.2K}{0.7K}))$ for the intermediate steps.

4. EXPERIMENTS AND RESULTS

Results are displayed in Tables 1 and 2. Best results are in bold, second best are underlined, and arrows indicate whether higher (\uparrow) or

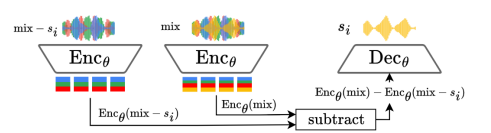


Figure 3: Oracle Music Source Separation via latent arithmetic.

lower (\downarrow) is better. Audio examples and supplementary material are available online 2 .

4.1. Experimental setup

Data: The training corpus is a large-scale music/speech dataset compiled from MTG-Jamendo [32], MoisesDB [33], M4Singer [34], DNS-Challenge [35], and E-GMD [36]. Tracks are sampled with weights (60, 20, 9, 8, 3) respectively, and a segment of 2 seconds is randomly cropped from each track. Segments are converted to mono and resampled to 44.1 kHz.

Baselines: We report metrics using the publicly available weights of Music2Latent (M2L-Pub) [4]. As a fairer baseline, we retrain M2L-Pub on the same data as our model, including the random gains and artificial mixtures for data augmentation, but without our proposed implicit homogeneity and additivity conditioning strategies (M2L). We also report metrics for the public weights from Stable Audio 1.0 VAE [11] (SA-VAE), serving as another autoencoder baseline with a different architecture and training procedure.

4.2. Reconstruction Quality

We evaluate the reconstruction quality of the AEs on 2-second audio chunks (0.5s overlap) from the MusicCaps dataset [37]. We reconstruct the full track using overlap-add and compute three metrics: (I) The Signal to Noise Ratio (SNR) on the waveform. (II) A Multi-Scale Spectral distance (MSS) between the original and reconstructed log-mel spectrograms using multiple resolutions³. (III) The Kernel Audio Distance (KAD) [38] between the embedding distributions of the original and reconstructed tracks⁴.

Table 2 summarizes the results. Our retrained baseline (M2L) already improves on the public M2L-Pub weights [4], likely due to our distinct training data, batch size and augmentations. The linearized model (Lin-CAE) remains notably comparable on MSS and improves further on SNR, indicating that our method does not degrade reconstruction fidelity. Compared to SA-VAE, Lin-CAE is slightly worse, a similar finding to [4,26]. We note that SA-VAE uses different data and a two-stage training procedure that optimizes both reconstruction and adversarial losses, while Lin-CAE is trained with a single denoising objective. KAD scores for Lin-CAE are better than our retrained M2L-Pub model and SA-VAE, but are worse than the public M2L weights (possibly reflecting the different training data distribution).

4.3. Homogeneity

We use the same data and setup as for reconstruction, but we additionally assess the model's ability to preserve scaling by drawing a random scalar a for each track x and measuring the ef-

²https://bernardo-torres.github.io/projects/linear-cae

 $^{^380}$ mel bands and hop lengths of $\approx 10, 25, \text{ and } 50 \text{ ms.}$

⁴Embedding distribution metrics have become a standard way of evaluating generative models, so we include it for completeness. KAD is computed using half of the reconstructed tracks, using the other half as the reference set. We use the kadtk library with the LAION-CLAP model.

Table 1: Additivit	y and oracle Music Source S	Separation using latent	space arithmetic on the MUSDB18-HQ data	iset.

	Additivity		Reconstruction		Separation								
	Dec	coder	Encoder	M	lix	I	Bass	D	rums	(Other	V	ocals
Model	$\overline{\text{MSS}}\downarrow$	SNR ↑	Error ↓	$\overline{\text{MSS}}\downarrow$	SNR ↑	$\overline{\text{MSS}}\downarrow$	SI-SDR ↑	$\overline{\text{MSS}}\downarrow$	SI-SDR ↑	$\overline{\text{MSS}}\downarrow$	SI-SDR ↑	$\overline{\text{MSS}}\downarrow$	SI-SDR ↑
M2L-Pub [4]	5.01	-0.79	2.82	1.16	-1.29	95.34	-14.85	28.08	-16.30	6.78	-16.11	5.10	-18.16
SA-VAE [11]	5.38	-12.58	1.71	0.57	4.03	323.26	-2.81	87.80	-3.11	3.65	-4.10	3.08	-4.48
M2L	5.21	-0.48	2.73	0.97	0.10	39.56	-11.11	12.26	-11.95	5.30	-11.81	3.49	-12.56
Lin-CAE	0.99	1.22	0.60	1.00	0.21	1.58	-0.59	1.16	-0.28	1.21	-1.82	1.23	-1.18
Ablations													
- Additivity	1.68	0.30	2.07	1.39	-0.06	6.61	-7.12	2.37	-6.11	3.44	-8.52	2.87	-12.18
- Homogeneity	4.24	-0.89	1.42	<u>0.96</u>	0.43	23.61	-5.96	7.84	-5.14	2.98	-8.30	3.08	-7.95

Table 2: MusicCaps Reconstruction and Homogeneity (Hom.).

	Recons	truction	Dec-	Hom.	Enc-Hom.	
Model	$\overline{MSS}\downarrow$	SNR ↑	$\overline{\text{MSS}}\downarrow$	SNR ↑	Error ↓	$KAD\downarrow$
M2L-Pub [4]	1.14	1.85	2.52	-4.69	12.13	5.69
SA-VAE [11]	0.72	7.32	3.03	-1.27	4.59	6.27
M2L	0.98	3.09	2.27	-2.30	8.52	6.53
Lin-CAE	1.01	3.19	1.37	0.86	0.69	6.19

fect on the output of both the encoder and decoder. We measure (I) **Encoder Homogeneity (Enc-Hom.)** as the relative L_2 error between the scaled input's latent and the latent of the scaled input: $\|\operatorname{Enc}_{\theta}(a \cdot x) - a \cdot \operatorname{Enc}_{\theta}(x)\|_2 / \|a \cdot \operatorname{Enc}_{\theta}(x)\|_2$. We employ a relative error to normalize for the smaller latent norms produced by models trained with homogeneity, which would make a standard L_2 comparison misleading; (II) **Decoder Homogeneity (Dec-Hom.)** as the SNR and MSS between $a \cdot \operatorname{Dec}_{\theta}(\mathbf{z}_x)$ and $\operatorname{Dec}_{\theta}(a \cdot \mathbf{z}_x)$.

Results are shown in Table 2, where it is shown that Lin-CAE achieves much better **decoder homogeneity** (Table 2) properties compared to both baselines. For all baselines, we see a significant degradation in reconstruction metrics when testing the effect of random gains, while our model is much more robust. A high degradation in the log-domain MSS indicates that the scaling of the latent translates to significant timbral changes in the output. Lin-CAE's MSS degrades less ($1.01 \rightarrow 1.37$) than the baselines (M2L: $0.98 \rightarrow 2.27$ and SA-VAE: $0.72 \rightarrow 3.03$). The **encoder** also exhibits significantly lower homogeneity errors compared to all baselines.

4.4. Additivity

Additivity is evaluated on four source mixtures from the Musdb18-HQ test set [39], where a mixture is: $\min = \sum_{i=1}^4 s_i$. s_i correspond to either vocals, bass, drum or other. We measure **Encoder Additivity Error** as the deviation of a mixture's latent from the sum of its source latents, calculated as the relative L_2 error: $\|\operatorname{Enc}_{\theta}(\min) - \sum_i \operatorname{Enc}_{\theta}(s_i)\|_2 / \|\operatorname{Enc}_{\theta}(\min)\|_2$. For **Decoder Additivity (Composability)**, we test the ability to reconstruct a mixture from the sum of its source latents by SNR and MSS between the decoded sum of latents, $\operatorname{Dec}_{\theta}(\sum_i \operatorname{Enc}_{\theta}(s_i))$, to the *autoencoded* mixture, $\operatorname{Dec}_{\theta}(\operatorname{Enc}_{\theta}(\min))$.

Our results (Table 1) show that Lin-CAE achieves a very low MSS (0.99) compared to the baselines (> 5), indicating that the summation in the latent space is very close to the autoencoded mixture, while the baselines produce a significantly degraded output. We encourage the reader to listen to the audio examples, as this is very clearly perceptible. The **encoder** also exhibits significantly lower additivity errors. Paired with the results from encoder homogeneity, this suggests that our implicit conditioning strategy encourages the

entire AE mapping to become more linear, not just the decoder.

4.5. Music source separation via latent arithmetic

We perform source separation via latent arithmetic on the Musdb18-HQ test set. A source \hat{s}_i is estimated by subtracting the latent representation of its accompaniment from the latent of the full mixture: $\hat{s}_i = \mathrm{Dec}_{\theta}(\mathrm{Enc}_{\theta}(\mathrm{mix}) - \mathrm{Enc}_{\theta}(\mathrm{mix} - s_i))$. Figure 3 illustrates this process. The quality of the separated source is evaluated against the *autoencoded* ground-truth source, $\mathrm{Dec}_{\theta}(\mathrm{Enc}_{\theta}(s_i))$, using Scale-invariant Signal to Distortion Ratio (SI-SDR) [40] and MSS.

Table 1 shows that Lin-CAE significantly outperforms the baselines in latent arithmetic/oracle source separation tasks, achieving higher SI-SDR and lower MSS scores by a large margin for every instrument. Notably, both separation metrics are of the same order of magnitude as the reconstruction values for the mix, which can be seen as an upper bound for the model. That is not the case, however, for any of the baselines, with the least significant gap for SA-VAE. We note that during training, we have only shown positive gains to the model, while during separation, we are effectively applying negative gains when subtracting latents. This further indicates the robustness of the learned linear structure.

Ablations: We retrain Lin-CAE with only one of the two properties (homogeneity or additivity) and report source separation results in Table 1. Performance in every metric degrades significantly when only one of the two properties is applied. Surprisingly, training with only homogeneity seems to help the additivity and source separation much more as a byproduct than training with only additivity.

5. CONCLUSION

We introduce a simple method to induce an approximately linear latent space in audio autoencoders during training. Using implicit conditioning via data augmentation, our approach enforces the properties of a linear map (homogeneity and additivity) without necessitating any modifications to the architecture or loss function. Experiments with Consistency Autoencoders (CAEs) show that linearization preserves high-quality reconstruction and can be used for source separation via latent arithmetic.

Our approach enables more interpretable and controllable audio generation. Future work could extend this method to improved CAE architectures [26] and downstream tasks like generative source separation [41]. Direct, low-level manipulations in compressed space promise new possibilities for audio editing and efficient signal processing.

6. REFERENCES

- Theodoros Kouzelis, Ioannis Kakogeorgiou, Spyros Gidaris, and Nikos Komodakis, "EQ-VAE: Equivariance regularized latent space for improved generative image modeling," arXiv preprint arXiv:2502.09509, 2025.
- [2] Ivan Skorokhodov, Sharath Girish, Benran Hu, Willi Menapace, Yanyu Li, Rameen Abdal, Sergey Tulyakov, and Aliaksandr Siarohin, "Improving the diffusability of autoencoders," arXiv preprint arXiv:2502.14831, 2025
- [3] Yifan Zhou, Zeqi Xiao, Shuai Yang, and Xingang Pan, "Alias-free latent diffusion models:improving fractional shift equivariance of diffusion latent space," arXiv preprint arXiv:2503.09419, 2025.
- [4] Marco Pasini, Stefan Lattner, and George Fazekas, "Music2Latent: Consistency autoencoders for latent audio compression," in *ISMIR*, San Francisco, USA, 2024, pp. 111–119.
- [5] Giovanni Bindi and Philippe Esling, "Unsupervised composable representations for audio," in *ISMIR*, San Francisco, USA, 2024, pp. 1037–1045.
- [6] Ahmed Omran, Neil Zeghidour, Zalán Borsos, Félix de Chaumont Quitry, Malcolm Slaney, and Marco Tagliasacchi, "Disentangling speech from surroundings with neural embeddings," in *ICASSP*, Rhodes, Greece, 2023, pp. 1–5.
- [7] Haoyang Li, Jia Qi Yip, Tianyu Fan, and Eng Siong Chng, "Speech enhancement using continuous embeddings of neural audio codec," in *ICASSP*, Hyderabad, India, 2025, pp. 1–5.
- [8] Dimitrios Bralios, Paris Smaragdis, and Jonah Casebeer, "Learning to upsample and upmix audio in the latent domain," arXiv preprint arXiv:2506.00681, 2025.
- [9] Dimitrios Bralios, Jonah Casebeer, and Paris Smaragdis, "Rebottleneck: Latent re-structuring for neural audio autoencoders," arXiv preprint arXiv:2507.07867, 2025.
- [10] Flavio Schneider, Ojasv Kamal, Zhijing Jin, and Bernhard Schölkopf, "Moûsai: Efficient text-to-music diffusion models," in ACL, Bangkok, Thailand, 2024, pp. 8050–8068.
- [11] Zach Evans, Julian D. Parker, CJ Carr, Zack Zukowski, Josiah Taylor, and Jordi Pons, "Stable audio open," in ICASSP. 2025, pp. 1–5, IEEE.
- [12] Javier Nistal, Marco Pasini, Cyran Aouameur, Maarten Grachten, and Stefan Lattner, "Diff-a-riff: Musical accompaniment co-creation via latent diffusion models," in *ISMIR*, San Francisco, USA, 2024, pp. 272–280.
- [13] Xiaoyu Bie, Xubo Liu, and Gaël Richard, "Learning source disentanglement in neural audio codec," in ICASSP, 2025, pp. 1–5.
- [14] Efthymios Tzinis, Shrikant Venkataramani, Zhepei Wang, Y. Cem Sübakan, and Paris Smaragdis, "Two-step sound source separation: Training on learned latent targets," in *ICASSP*. 2020, pp. 31–35, IEEE.
- [15] Jonathan Ho, Ajay Jain, and Pieter Abbeel, "Denoising diffusion probabilistic models," in *NeurIPS*, 2020.
- [16] Yang Song, Jascha Sohl-Dickstein, Diederik P. Kingma, Abhishek Kumar, Stefano Ermon, and Ben Poole, "Score-based generative modeling through stochastic differential equations," in *ICLR*, 2021.
- [17] Yang Song, Prafulla Dhariwal, Mark Chen, and Ilya Sutskever, "Consistency models," in *ICML*, 2023, pp. 32211–32252.
- [18] Yang Song and Prafulla Dhariwal, "Improved techniques for training consistency models," arXiv preprint arXiv:2310.14189, 2023.
- [19] Alexandre Défossez, Jade Copet, Gabriel Synnaeve, and Yossi Adi, "High fidelity neural audio compression," 2023.
- [20] Diederik P. Kingma and Max Welling, "Auto-encoding variational bayes," in *ICLR*, Yoshua Bengio and Yann LeCun, Eds., 2014.
- [21] Patrick Esser, Robin Rombach, and Björn Ommer, "Taming transformers for high-resolution image synthesis," in CVPR, 2021, pp. 12873–12883.

- [22] Konpat Preechakul, Nattanat Chatthee, Suttisak Wizadwongsa, and Supasorn Suwajanakorn, "Diffusion autoencoders: Toward a meaningful and decodable representation," in CVPR, New Orleans, USA, 2022, pp. 10609–10619.
- [23] Vighnesh Birodkar, Gabriel Barcik, James Lyon, Sergey Ioffe, David Minnen, and Joshua V. Dillon, "Sample what you cant compress," arXiv preprint arXiv:2409.02529, 2024.
- [24] Yinbo Chen, Rohit Girdhar, Xiaolong Wang, Sai Saketh Rambhatla, and Ishan Misra, "Diffusion autoencoders are scalable image tokenizers," arXiv preprint arXiv:2501.18593, 2025.
- [25] Long Zhao, Sanghyun Woo, Ziyu Wan, Yandong Li, Han Zhang, Bo-qing Gong, Hartwig Adam, Xuhui Jia, and Ting Liu, "Epsilon-vae: Denoising as visual decoding," arXiv preprint arXiv:2410.04081, 2024.
- [26] Marco Pasini, Stefan Lattner, and György Fazekas, "Music2Latent2: Audio compression with summary embeddings and autoregressive decoding," in *ICASSP*, Hyderabad, India, 2025, pp. 1–5.
- [27] Julius Richter, Simon Welker, Jean-Marie Lemercier, Bunlong Lay, and Timo Gerkmann, "Speech enhancement and dereverberation with diffusion-based generative models," *TASLP*, vol. 31, pp. 2351–2364, 2023.
- [28] Ge Zhu, Yutong Wen, Marc-André Carbonneau, and Zhiyao Duan, "Edmsound: Spectrogram based diffusion models for efficient and high-quality audio synthesis," arXiv preprint arXiv:2311.08667, 2023.
- [29] Tero Karras, Miika Aittala, Timo Aila, and Samuli Laine, "Elucidating the design space of diffusion-based generative models," in *NeurIPS*, 2022, vol. 35, pp. 26565–26577.
- [30] Scott Wisdom, Efthymios Tzinis, Hakan Erdogan, Ron J. Weiss, Kevin W. Wilson, and John R. Hershey, "Unsupervised sound separation using mixture invariant training," in *NeurIPS*, 2020.
- [31] Pierre Charbonnier, Laure Blanc-Féraud, Gilles Aubert, and Michel Barlaud, "Deterministic edge-preserving regularization in computed imaging," *IEEE Trans.on Image Processing*, vol. 6, no. 2, pp. 298–311, 1997.
- [32] Dmitry Bogdanov, Minz Won, Philip Tovstogan, Alastair Porter, and Xavier Serra, "The MTG-jamendo dataset for automatic music tagging," in MLMD Workshop @ ICML, Long Beach, CA, US, 2019.
- [33] Igor Pereira, Felipe Araújo, Filip Korzeniowski, and Richard Vogl, "MoisesDB: A dataset for source separation beyond 4-stems," in *ISMIR*, 2023, pp. 619–626.
- [34] Lichao Zhang, Ruiqi Li, Shoutong Wang, Liqun Deng, Jinglin Liu, Yi Ren, Jinzheng He, Rongjie Huang, Jieming Zhu, Xiao Chen, et al., "M4Singer: A multi-style, multi-singer and musical score provided mandarin singing corpus," in *NeurIPS*, 2022, vol. 35, pp. 6914–6926.
- [35] Harishchandra Dubey, Ashkan Aazami, Vishak Gopal, Babak Naderi, Sebastian Braun, Ross Cutler, Hannes Gamper, Mehrsa Golestaneh, and Robert Aichner, "ICASSP 2023 deep noise suppression challenge," in ICASSP, Rhodes, Greece, 2023.
- [36] Lee Callender, Curtis Hawthorne, and Jesse Engel, "Improving perceptual quality of drum transcription with the expanded groove MIDI dataset," arXiv preprint arXiv:2004.00188, 2020.
- [37] Andrea Agostinelli, Timo I. Denk, Zalán Borsos, Jesse Engel, Mauro Verzetti, Antoine Caillon, Qingqing Huang, Aren Jansen, Adam Roberts, Marco Tagliasacchi, Matt Sharifi, Neil Zeghidour, and Christian Frank, "MusicLM: Generating Music From Text," Jan. 2023.
- [38] Yoonjin Chung, Pilsun Eu, Junwon Lee, Keunwoo Choi, Juhan Nam, and Ben Sangbae Chon, "KAD: No more FAD! An effective and efficient evaluation metric for audio generation," arXiv preprint arXiv:2502.15602, 2025.
- [39] Zafar Rafii, Antoine Liutkus, Fabian-Robert Stöter, Stylianos Ioannis Mimilakis, and Rachel Bittner, "MUSDB18-HQ - an uncompressed version of MUSDB18," Aug. 2019.
- [40] Jonathan Le Roux, Scott Wisdom, Hakan Erdogan, and John R Hershey, "SDR-half-baked or well done?," in *ICASSP*, Brighton, UK, 2019, pp. 626–630. IEEE.
- [41] Giorgio Mariani, Irene Tallini, Emilian Postolache, Michele Mancusi, Luca Cosmo, and Emanuele Rodolà, "Multi-source diffusion models for simultaneous music generation and separation," in ICLR, 2024.